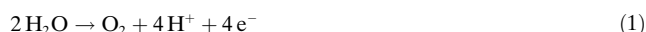


Calcium Manganese(III) Oxides ($\text{CaMn}_2\text{O}_4 \cdot x\text{H}_2\text{O}$) as Biomimetic Oxygen-Evolving Catalysts**

Mohammad Mahdi Najafpour, Till Ehrenberg, Mathias Wiechen, and Philipp Kurz*

Light-driven water splitting into hydrogen and oxygen is currently intensely discussed as an option for the conversion of solar energy into a “solar fuel”.^[1–3] One of the great challenges to make such a proposal a reality is the development of efficient catalysts from abundant resources for Reaction (1), the oxidation of water to molecular oxygen.



To achieve this goal, natural photosynthesis has been taken as an inspiration, in which light-driven water oxidation is catalyzed by the μ -oxido- Mn_4Ca cluster of the oxygen-evolving complex (OEC) of photosystem II (PSII).^[3–7]

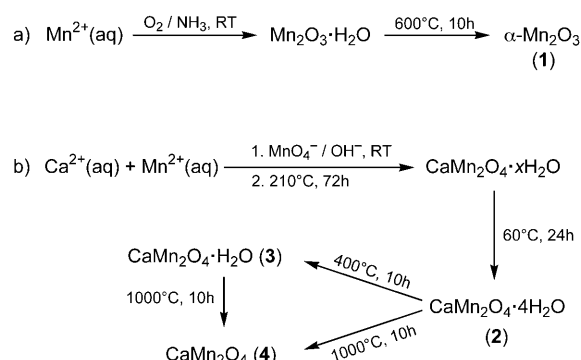
To date, efforts to synthesize functional manganese mimics of the OEC have mainly focused on a “bottom-up” approach: μ -oxido manganese complexes with two (and, much more rarely, three or four) manganese centers were prepared and their properties studied in great detail.^[8,9] However, a true water-oxidation catalyst could not be found among these manganese complexes. All manganese compounds tested to date for their catalytic properties require the use of oxygen-transfer and/or two-electron oxidizing agents to catalyze the formation of oxygen in homogeneous solution.^[3,5,9–11] The OEC, in comparison, efficiently catalyzes Reaction (1) after fourfold single-electron removal by an oxidized tyrosine residue (Y_Z^+) of PSII.^[3–5]

Herein, we present a “top-down” approach to biomimetic water oxidation and show that manganese oxide and calcium manganese oxide particles are active catalysts for Reaction (1). By doing so, we follow previous work, which indicated that manganese hydroxides and oxides were promising catalysts for water oxidation in both photochemical^[12,13] and electrochemical^[14–16] systems. It was shown for

oxides used as electrocatalysts that the performances of materials containing manganese in the +III oxidation state was superior to pure $\text{Mn}^{\text{IV}}\text{O}_2$, which suggests that Mn^{III} sites on the oxide surfaces might be the catalytically active species.^[15,16]

First, we will present the catalytic properties of manganese(III) oxide particles ($\alpha\text{-Mn}_2\text{O}_3$). Thereafter, we turn our attention to calcium manganese(III) oxide hydrates, $\text{CaMn}_2\text{O}_4 \cdot x\text{H}_2\text{O}$, with the aim of investigating an oxide system that is even more closely related to the elemental composition of the $\text{Mn}_4\text{O}_x\text{Ca}$ core of the OEC.

We originally suspected that the rather slow catalysis of Reaction (1) by Mn_2O_3 described previously might have been due to the small surface area of about $1\text{ m}^2\text{ g}^{-1}$ of the Mn_2O_3 used.^[13] Therefore, synthetic routes to prepare particles of $\alpha\text{-Mn}_2\text{O}_3$ and $\text{CaMn}_2\text{O}_4 \cdot x\text{H}_2\text{O}$ with enhanced surface areas were developed, which was achieved by carefully oxidizing manganese(II) ions in basic aqueous solutions with or without additional calcium ions present (Scheme 1; see the Support-



Scheme 1. The preparation of a) $\alpha\text{-Mn}_2\text{O}_3$ and b) $\text{CaMn}_2\text{O}_4 \cdot x\text{H}_2\text{O}$ particles in aqueous solution.

ing Information for details). The freshly precipitated, mildly dried oxide materials contain significant amounts of water, as indicated by IR/Raman spectroscopy (Supporting Information, Figure S1) and a determination of the manganese content by atomic absorption spectroscopy (AAS). Heating the materials to 600°C (for $\text{Mn}_2\text{O}_3 \cdot \text{H}_2\text{O}$) or 400°C (for $\text{CaMn}_2\text{O}_4 \cdot 4\text{H}_2\text{O}$, **2**) results in dehydration (Supporting Information, Figure S2) and the formation of oxides with the homogeneous elemental compositions Mn_2O_3 (**1**) or $\text{CaMn}_2\text{O}_4 \cdot \text{H}_2\text{O}$ (**3**), respectively (see Supporting Information for IR, Raman, AAS, and EDX data).

To characterize the morphology of the prepared oxides, we studied the products by scanning electron microscopy (SEM), which indicated powders with particles circa $5\text{--}50\text{ }\mu\text{m}$

[*] Dr. M. M. Najafpour,^[‡] T. Ehrenberg, M. Wiechen, Dr. P. Kurz
Institute for Inorganic Chemistry, Christian-Albrechts-University Kiel
Max-Eyth-Strasse 2, 24118 Kiel (Germany)
Fax: (+49) 431-880-1520
E-mail: phkurz@ac.uni-kiel.de
Homepage: www.ac.uni-kiel.de/phkurz

[†] Current address: Institute for Advanced Studies in Basic Sciences (IASBS), Zanjan (Iran)

[**] The authors would like to thank Ursula Cornelissen, Bastian Dietl, Kathrin Gerwien, Joachim Gripp, Jannes Ophay, Enrique Quiroga, Monika Schneeweiß, Christian Stoltenberg, and Adam Wutkowski (all CAU Kiel) for experimental support. M.M.N. thanks the Ministry of Science and the National Elite Foundation of Iran for a travel grant. This work was financed by the Fonds der Chemischen Industrie (Liebig fellowship for P.K.).

Supporting information for this article is available on the WWW under <http://dx.doi.org/10.1002/anie.200906745>.

in size (Figure 1). The results of nitrogen surface adsorption experiments confirmed that our preparation methods indeed yielded oxides of greatly increased surface areas: BET analysis determined S_{BET} as $16.6 \text{ m}^2 \text{ g}^{-1}$ for Mn_2O_3 (**1**), in contrast to $1.09 \text{ m}^2 \text{ g}^{-1}$ found for commercially available Mn_2O_3 (similar to the material of reference [13]). For the synthesized $\text{CaMn}_2\text{O}_4 \cdot x\text{H}_2\text{O}$, we found an even larger surface per mass (Table 1), with $303 \text{ m}^2 \text{ g}^{-1}$ (**2**) and $205 \text{ m}^2 \text{ g}^{-1}$ (**3**).

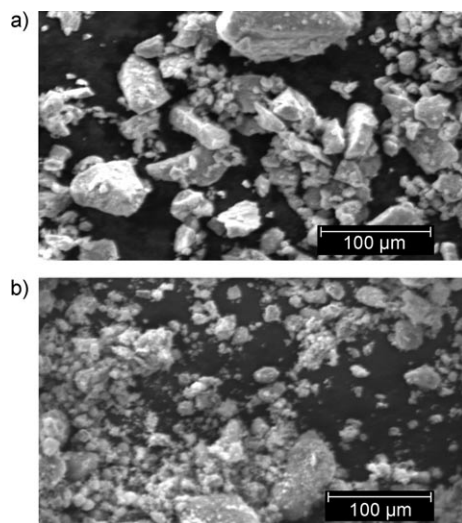


Figure 1. SEM micrographs of a) $\alpha\text{-Mn}_2\text{O}_3$ (**1**) and b) $\text{CaMn}_2\text{O}_4 \cdot \text{H}_2\text{O}$ (**3**) prepared for the oxygen-evolving catalysis study.

Table 1: Oxygen evolution rates [$\text{mmol O}_2 \text{ mol}_{\text{Mn}}^{-1} \text{ s}^{-1}$] determined by Clark electrode detection.

Catalyst	$S_{\text{BET}}^{[b]}$	H_2O_2	Oxidation agent ^[a]		$\text{Ru}^{\text{III}}_{\text{photo}}^{[c]}$
			HSO_5^-	Ce^{IV}	
commercial Mn_2O_3	1.09	0.3	traces	traces	0.022
$\alpha\text{-Mn}_2\text{O}_3$ (1)	16.6	0.2	traces	0.027	0.023
$\text{CaMn}_2\text{O}_4 \cdot 4\text{H}_2\text{O}$ (2)	303	$> 5.0^{[d]}$	0.325	0.325	0.325
$\text{CaMn}_2\text{O}_4 \cdot \text{H}_2\text{O}$ (3)	205	4.2	0.255	0.540	0.350
CaMn_2O_4 (4)	2.62	0.9	0.024	traces	0.012
$\text{CaMn}_2\text{O}_4 \cdot 4\text{H}_2\text{O}$ (5)	14.8	$> 5.0^{[d]}$	0.012	0.290	0.225

[a] Concentrations of the oxidants in the reaction mixture (1 mL): $[\text{H}_2\text{O}_2] = 4.4 \text{ mM}$, $[\text{HSO}_5^-] = 7.4 \text{ mM}$, $[\text{Ce}^{\text{IV}}] = 0.24 \text{ M}$, $[\text{Ru}(\text{bipy})_3]^{2+} = 1.5 \text{ mM}$, $[\text{Co}(\text{NH}_3)_5\text{Cl}]^{2+} = 12.5 \text{ mM}$. [b] Values in $\text{m}^2 \text{ g}^{-1}$. [c] Rates for the phase of steady O_2 formation (2–3 min. after the start of the illumination). [d] Rate faster than the upper detection limit of the setup of circa $5 \text{ mmol O}_2 \text{ mol}_{\text{Mn}}^{-1} \text{ s}^{-1}$.

X-ray powder diffractometry (XRD) was used to identify the formed oxide phases. As expected from the Mn–O phase diagram and previous reports,^[17,18] the manganese(III) oxide **1** was obtained from the synthesis as $\alpha\text{-Mn}_2\text{O}_3$ (Figure 2). The materials **2** and **3** obtained in the calcium manganese oxide preparation were amorphous, and a phase could therefore not be identified. However, heating of the material to 1000°C yielded marokite (CaMn_2O_4 , **4**), a naturally occurring mineral discovered in Morocco in 1963.^[19] Both $\alpha\text{-Mn}_2\text{O}_3$ and marokite contain structural elements suggested for the architecture of the OEC,^[3] which makes both very interesting

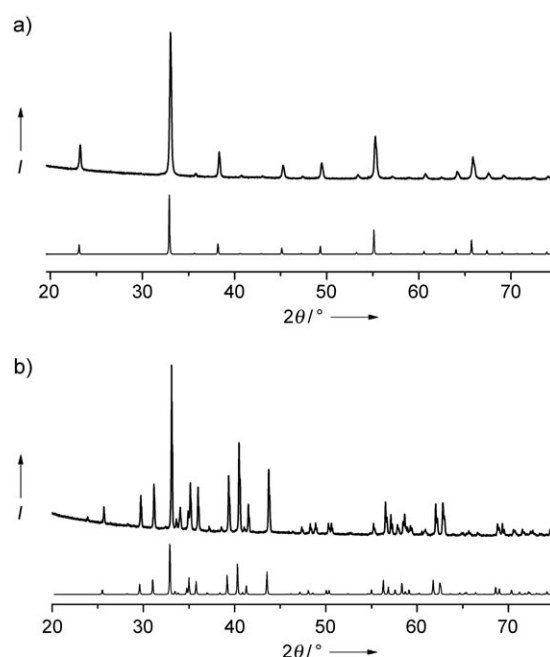


Figure 2. Powder XRD for a) Mn_2O_3 (**1**) and b) CaMn_2O_4 (**4**) prepared according to Scheme 1. The lower curves below each of the patterns indicate the expected Bragg reflections for $\alpha\text{-Mn}_2\text{O}_3$ and marokite, respectively.

models for the $\text{Mn}_4\text{O}_x\text{Ca}$ catalytic site of PSII (Supporting Information, Figure S3 and S4).

From the analytical data, we concluded that the syntheses as presented in Scheme 1 yield manganese(III) and calcium–manganese(III) oxide particles with defined compositions and high surface areas.

We then investigated the ability of the oxides to act as oxygen-evolving catalysts using a well-established experimental setup.^[11] Aqueous suspensions of the oxides were prepared in the measurement cell of a Clark-type polarographic oxygen electrode. The dissolved oxygen was removed by argon purging, before solutions of three different, strong oxidation agents (H_2O_2 , HSO_5^- , or Ce^{IV}) were added to the cell. The formation of oxygen was then followed (Figure 3, 4, and Supporting Information, Figure S5) and O_2 formation rates per manganese center were obtained from linear fits of the data (Table 1).

As expected for manganese oxides, Clark electrode detection demonstrated that all the materials were efficient catalysts for the disproportionation reaction of H_2O_2 into O_2 and H_2O . Oxygen formation was also observed for reactions with the two-electron oxygen-transfer oxidant HSO_5^- (oxone), which has been frequently used in OEC model chemistry^[11,20] (Table 1 and Supporting Information, Figure S5). Gas chromatography measurements for the headspace above suspensions of the most efficient catalysts (**1** and **3**) confirmed these results (Supporting Information, Figure S6).

Although the formation of oxygen in reactions with H_2O_2 and HSO_5^- is well known for dinuclear manganese complexes, no manganese complex has been found to date that is able to catalyze oxygen evolution in homogeneous solution

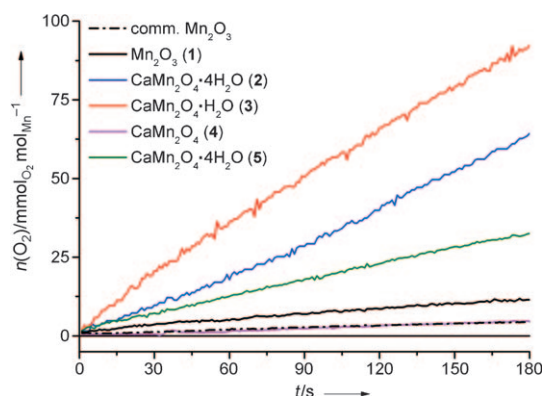


Figure 3. Oxygen evolution traces for the reactions of different (calcium) manganese oxides with cerium(IV) added to oxide suspensions at $t = 0$ s. Curves for **1**, **4**, and commercially available Mn_2O_3 are magnified fivefold.

when oxidized by the strong one-electron oxidation agent cerium(IV) [$E_0 \approx +1.7$ V vs. NHE in acidic solution^[21]]. As cerium(IV) does not act as oxygen-transfer reagent, these reactions are model reactions for true water oxidation and have been studied in great detail for the case of the blue ruthenium dimer $[(\text{bpy})_2(\text{H}_2\text{O})\text{Ru}^{\text{III}}(\mu\text{-O})\text{ORu}^{\text{III}}(\text{H}_2\text{O})(\text{bpy})_2]^{4+}$ acting as water-oxidation catalyst.^[22,23]

Herein, all the batches of Mn_2O_3 and $\text{CaMn}_2\text{O}_4 \cdot x\text{H}_2\text{O}$ that were studied catalyzed this reaction (Figure 3 and Table 1). Again, catalysis was efficient for the hydrated calcium manganese oxides and the rate of oxygen evolution was constant for extended periods of time. Much less O_2 was formed in reactions of cerium(IV) with Mn_2O_3 or marokite (**4**). To confirm that the differences in reaction rates were not merely effects of the different surface areas of the materials, we modified the synthetic procedure and prepared a $\text{CaMn}_2\text{O}_4 \cdot 4\text{H}_2\text{O}$ (**5**) with a surface area of only $14.8 \text{ m}^2 \text{ g}^{-1}$, which is comparable to Mn_2O_3 (**1**). Again, the calcium manganese oxide **5** showed a much higher activity per manganese center in comparison to **1**.

We were also able to confirm these results by GC detection of the O_2 reaction product. Oxygen evolved at a continuous rate for both Mn_2O_3 and the calcium manganese oxide **3**, but within 60 minutes, about 30 times more O_2 per manganese atom was formed in the reaction of cerium(IV) with **3** than for the same reaction with **1** (Table 2 and Supporting Information, Figure S6).

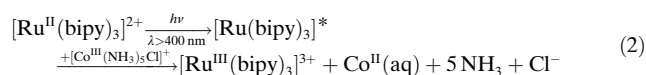
Table 2: Total oxygen [$\text{mmol O}_2 \text{ mol Mn}^{-1}$] in the headspace above oxide suspensions after a reaction time of 1 hour.

catalyst	H_2O_2	Oxidation agent ^[a]		$\text{Ru}^{\text{III}}_{\text{photo}}$
		HSO_5^-	Ce^{IV}	
$\alpha\text{-Mn}_2\text{O}_3$ (1)	0.10 ^[b]	0.15	0.03	n.q. ^[c]
$\text{CaMn}_2\text{O}_4 \cdot \text{H}_2\text{O}$ (3)	0.18 ^[b]	0.12	0.90	n.q. ^[c]

[a] Reaction mixtures contained **1** and **3** (1 mg mL^{-1}) and oxidation agents in the same concentrations as given in the footnote to Table 1. [b] Data for reaction times of only 30 min. [c] O_2 detected by GC, but no reproducible quantification possible as the photooxidation system is not stable for longer time periods.

It is difficult to translate the figures of Table 2 into turnover numbers, as both the fraction of accessible manganese/calcium atoms on the oxide surface and the number of manganese/calcium centers that constitute one catalytic unit is unknown. Nevertheless, we tried to estimate the number of manganese atoms on the surface with a simple model and estimated this fraction to be one in six for **3** and one in fifty for **1** (Supporting Information, Figure S7). As it is unlikely that every single manganese atom on the surface should be an individual catalytic site, we therefore consider all the reactions in Table 2 to be catalytic by the criterion of reaching more than one turnover per site, but we are of course unable to determine absolute turnover numbers.

Encouraged by the good catalytic performances of the oxide materials found in the experiments with cerium(IV), we went a step further and investigated light-driven reactions with the aim of studying a model for a PS II-like photo-redox chain. We used the $[\text{Ru}^{\text{II}}(\text{bipy})_3]^{2+}/[\text{Co}^{\text{III}}(\text{NH}_3)_5\text{Cl}]^{2+}$ system in which the strong single-electron oxidation agent $[\text{Ru}^{\text{III}}(\text{bipy})_3]^{3+}$ ($E_0 \approx +1.3$ V) is generated by visible-light illumination according to Reaction (2):



The photooxidation reactions were carried out in acetate buffer (pH 4), as Reaction (2) generates 5 equivalents of ammonia per ruthenium(III) in solution, and basic conditions are known to result in the fast degradation of the ruthenium photosensitizer.^[24]

Upon illumination with visible light ($\lambda > 400 \text{ nm}$), the formation of oxygen was observed (Figure 4). In an initial phase of 2–3 minutes, O_2 formation is slow while reaction (2) builds up a significant concentration of $[\text{Ru}^{\text{III}}(\text{bipy})_3]^{3+}$, which is detectable as the solution turns dark owing to the dark green ruthenium(III) compound formed. Steady rates of oxygen formation, which were again much higher for $\text{CaMn}_2\text{O}_4 \cdot x\text{H}_2\text{O}$ than for Mn_2O_3 , were then observed over approximately the next five minutes. Oxygen could also be detected by headspace GC; however, a reliable quantification

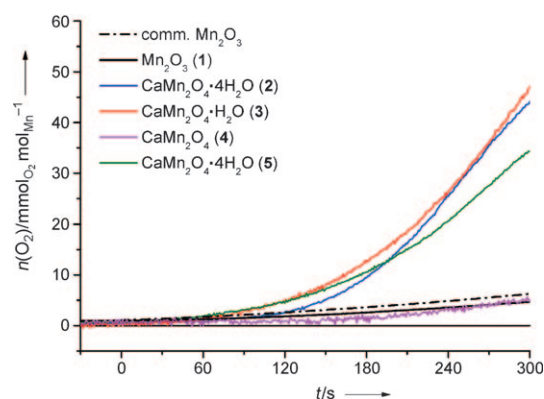


Figure 4. Oxygen evolution traces for the reactions of different (calcium) manganese oxides with photogenerated $[\text{Ru}^{\text{III}}(\text{bipy})_3]^{3+}$. Illumination was started at $t = 0$ s. Graphs for **1**, **4**, and commercially available Mn_2O_3 are magnified fivefold.

of the O₂ was not possible, as reaction rates for longer time periods were highly irreproducible. It is known from the literature that [Ru(bipy)₃] photooxidation systems decompose over time, and many factors (pH, reactant concentrations, buffer type, etc.) influence their reactivity.^[25–27] Furthermore, we found that the calcium manganese oxide catalysts are not stable for longer reaction times in commonly used acetate buffer. Despite these points, the photooxidation experiments presented herein are a clear proof-of-concept that light-driven water oxidation is possible using CaMn₂O₄·xH₂O, with initial rates well exceeding those achieved using Mn₂O₃.

To probe the stability of the oxide particles themselves, we exposed oxides **1** and **3** to the different oxidation agents for 60 minutes at conditions identical to catalysis runs and analyzed the resulting suspensions for dissolved metal ions. Only negligible amounts of manganese (<1% of the total amount) dissolved under any of the studied reaction conditions, even in the strongly acidic media containing HSO₅[–] or cerium(IV) (Supporting Information, Table S2). In contrast, a much larger fraction of the calcium (1–20% of the total) was found in solution after exposing **3** to catalysis conditions, with nearly half of the total calcium in solution after the photochemical reaction of **3** (46% dissolved Ca²⁺). We suspect that the presence of chelating acetate ligands from the buffer facilitates dissolution. However, in all cases for which we could quantify O₂, the total amount of O₂ formed (Table 2) by far exceeded the amount of dissolved oxide, thus demonstrating that O₂ formation is not linked to oxide dissolution.

XRD measurements of oxides **1** and **4** recovered from the suspensions after exposure to the oxidants also showed that the solid materials did not change but could still be identified as α-Mn₂O₃ and marokite, respectively (Supporting Information, Figure S8).

From the presented data, we conclude that both manganese(III) and calcium manganese(III) oxide particles are active catalysts for water oxidation. Whilst increased surface areas enhanced catalytic activity only marginally, the incorporation of calcium greatly improved the performances of these heterogeneous catalyst materials in comparison to the known system using Mn₂O₃. The presence of aquo- or hydroxo- groups on the surface also affects catalysis, as the hydrates **2**, **3**, and **5** are much more active than anhydrous marokite (CaMn₂O₄, **4**).

The results have important implications for the research on biomimetic water oxidation:

1) Calcium manganese oxides are very promising candidates to act as water-oxidation catalysts for artificial photosynthesis, demonstrated herein by using the well-known single-electron oxidation agents cerium(IV) and [Ru^{III}(bipy)₃]³⁺. The CaMn₂O₄·xH₂O oxide materials of this study can be easily synthesized from cheap and abundant starting materials. Together with the recently discovered cobalt systems,^[28,29] calcium manganese oxides are therefore much more suitable for potential large-scale applications than the well-studied, but expensive, IrO₂, RuO₂, and Rh₂O₃ catalysts.^[13,24]

2) The role of calcium in natural water oxidation catalysis (calcium(II)-depleted PSII is much less active than wild

type)^[30,31] can be reproduced by the rather simple model of a mixed calcium manganese oxide. Calcium has been suggested as binding and activation site for H₂O in the OEC; both roles of calcium can be envisioned for the reactions of CaMn₂O₄·xH₂O presented herein as well.

3) Finally, our results support earlier proposals suggesting that billions of years ago, the PSII proto-enzyme might have originated from naturally occurring manganese oxide minerals.^[32–34]

Received: November 30, 2009

Published online: February 22, 2010

Keywords: bioinorganic chemistry · heterogeneous catalysis · manganese · oxidation · water chemistry

- [1] N. Armaroli, V. Balzani, *Angew. Chem.* **2007**, *119*, 52–67; *Angew. Chem. Int. Ed.* **2007**, *46*, 52–66.
- [2] N. S. Lewis, D. G. Nocera, *Proc. Natl. Acad. Sci. USA* **2006**, *103*, 15729–15735.
- [3] W. Lubitz, E. J. Reijerse, J. Messinger, *Energy Environ. Sci.* **2008**, *1*, 15–31.
- [4] R. Lomoth, A. Magnuson, M. Sjödin, P. Huang, S. Styring, L. Hammarström, *Photosynth. Res.* **2006**, *87*, 25–40.
- [5] C. W. Cady, R. H. Crabtree, G. W. Brudvig, *Coord. Chem. Rev.* **2008**, *252*, 444–455.
- [6] C. Herrero, B. Lassalle-Kaiser, W. Leibl, A. W. Rutherford, A. Aukauloo, *Coord. Chem. Rev.* **2008**, *252*, 456–468.
- [7] C. S. Mullins, V. L. Pecoraro, *Coord. Chem. Rev.* **2008**, *252*, 416–443.
- [8] M. Yagi, M. Kaneko, *Chem. Rev.* **2001**, *101*, 21–35.
- [9] S. Mukhopadhyay, S. K. Mandal, S. B. Bhaduri, W. H. Armstrong, *Chem. Rev.* **2004**, *104*, 3981–4026.
- [10] Y. Shimazaki, T. Nagano, H. Takesue, B. H. Ye, F. Tani, Y. Naruta, *Angew. Chem.* **2004**, *116*, 100–102; *Angew. Chem. Int. Ed.* **2004**, *43*, 98–100.
- [11] P. Kurz, G. Berggren, M. F. Anderlund, S. Styring, *Dalton Trans.* **2007**, 4258–4261.
- [12] G. L. Elizarova, G. M. Zhidomirov, V. N. Parmon, *Catal. Today* **2000**, *58*, 71–88.
- [13] A. Harriman, I. J. Pickering, J. M. Thomas, P. A. Christensen, *J. Chem. Soc. Faraday Trans. 1* **1988**, *84*, 2795–2806.
- [14] Y. Matsumoto, E. Sato, *Mater. Chem. Phys.* **1986**, *14*, 397–426.
- [15] M. Morita, C. Iwakura, H. Tamura, *Electrochim. Acta* **1979**, *24*, 357–362.
- [16] S. Trasatti, *J. Electroanal. Chem.* **1980**, *111*, 125–131.
- [17] N. Chandra, S. Bhasin, M. Shanna, D. Pal, *Mater. Lett.* **2007**, *61*, 3728–3732.
- [18] S. Fritsch, A. Navrotsky, *J. Am. Ceram. Soc.* **1996**, *79*, 1761–1768.
- [19] C. Gaudefroy, G. Jouravsky, F. Permingeat, *Bull. Soc. Fr. Mineral. Cristallogr.* **1965**, *86*, 359–367.
- [20] H. Y. Chen, R. Tagore, G. Olack, J. S. Vrettos, T. C. Weng, J. Penner-Hahn, R. H. Crabtree, G. W. Brudvig, *Inorg. Chem.* **2007**, *46*, 34–43.
- [21] A. F. Holleman, E. Wiberg, *Lehrbuch der Anorganischen Chemie*, de Gruyter, Berlin, **1995**.
- [22] J. K. Hurst, *Coord. Chem. Rev.* **2005**, *249*, 313–328.
- [23] F. Liu, J. J. Concepcion, J. W. Jurss, T. Cardolaccia, J. L. Templeton, T. J. Meyer, *Inorg. Chem.* **2008**, *47*, 1727–1752.
- [24] N. D. Morris, T. E. Mallouk, *J. Am. Chem. Soc.* **2002**, *124*, 11114–11121.
- [25] A. Harriman, M. C. Richoux, P. A. Christensen, S. Mosseri, P. Neta, *J. Chem. Soc. Faraday Trans. 1* **1987**, *83*, 3001–3014.

- [26] P. G. Hoertz, T. E. Mallouk, *Inorg. Chem.* **2005**, *44*, 6828–6840.
 - [27] K. Kalyanasundaram, O. Micic, E. Pramauro, M. Grätzel, *Helv. Chim. Acta* **1979**, *62*, 2432–2441.
 - [28] F. Jiao, H. Frei, *Angew. Chem.* **2009**, *121*, 1873–1876; *Angew. Chem. Int. Ed.* **2009**, *48*, 1841–1844.
 - [29] M. W. Kanan, D. G. Nocera, *Science* **2008**, *321*, 1072–1075.
 - [30] D. F. Ghanotakis, G. T. Babcock, C. F. Yocum, *FEBS Lett.* **1984**, *167*, 127–130.
 - [31] M. Miyao, N. Murata, *FEBS Lett.* **1984**, *168*, 118–120.
 - [32] F. A. Armstrong, *Philos. Trans. R. Soc. London* **2007**, *363*, 1263–1270.
 - [33] K. Sauer, V. K. Yachandra, *Proc. Natl. Acad. Sci. USA* **2002**, *99*, 8631–8636.
 - [34] L. Spiccia, W. H. Casey, *Geochim. Cosmochim. Acta* **2007**, *71*, 5590–5604.
-